


Energy, Momentum, and Angular Momentum Transfer between Electrons and Nuclei

Chen Li^{1,2,3,*}, Ryan Requist^{1,2}, and E. K. U. Gross^{1,2}

¹Max Planck Institute of Microstructure Physics, Weinberg 2, 06120 Halle, Germany

²Fritz Haber Center for Molecular Dynamics, Institute of Chemistry, The Hebrew University of Jerusalem, Jerusalem 91904, Israel

³Beijing National Laboratory for Molecular Sciences, College of Chemistry and Molecular Engineering, Peking University, Beijing 100871, China

 (Received 12 August 2019; revised 12 January 2022; accepted 11 February 2022; published 17 March 2022)

The recently developed exact factorization approach condenses all electronic effects on the nuclear subsystem into scalar and vector potentials that appear in an effective time dependent Schrödinger equation. Starting from this equation, we derive subsystem Ehrenfest identities characterizing the energy, momentum, and angular momentum transfer between electrons and nuclei. An effective electromagnetic force operator induced by the electromagnetic field corresponding to the effective scalar and vector potentials appears in all three identities. The effective magnetic field has two components that can be identified with the Berry curvature calculated with (a) different Cartesian coordinates of the same nucleus and (b) arbitrary Cartesian coordinates of two different nuclei. (a) has a classical interpretation as the induced magnetic field felt by the nucleus, while (b) has no classical analog. Subsystem Ehrenfest identities are ideally suited for quantifying energy transfer in electron-phonon systems. With two explicit examples we demonstrate the usefulness of the new identities.

DOI: [10.1103/PhysRevLett.128.113001](https://doi.org/10.1103/PhysRevLett.128.113001)

The immensity of information in the quantum mechanical wave function is an obstacle to finding a clear physical picture of microscale dynamical processes. It is thus crucial to single out a few variables that condense the most relevant information, and experience shows this is particularly successful when these variables have classical analogs. This line of thinking dates back to Ehrenfest. For a single particle described by a time dependent Schrödinger equation (TDSE), the Ehrenfest theorem bridges the quantum and classical pictures by providing equations of motion for the expectation values of position and momentum that have a strong resemblance to Newton's equations [1].

Yet, real world systems are made up of multiple particle species. In this respect, the Ehrenfest theorem are limited because they do not probe the multicomponent nature of the system. It would therefore be desirable to go beyond the Ehrenfest theorem in the following two ways: (i) identifying useful variables that are specific to a subsystem, and (ii) deriving their equations of motion in a form which brings to light the classical analogs they contain.

For molecules and solids, three obvious candidates for (i) are the kinetic energy, momentum, and angular momentum of the nuclei. These variables are helpful in

gaining insight into dynamical phenomena where energy and momentum are transferred between electrons and nuclei. For example, energy transfer is crucial for understanding the fast internal conversion of DNA and RNA [2,3] and electronic friction-induced relaxation of molecular vibrations [4–6]. By tuning the energy transfer rate, one can control current-induced forces [7–9] in nano-systems and minimize Joule heating [10,11]. By understanding angular momentum transfer on the microscale, one may find inspiration in designing molecular motors and refrigerators [12–15] and in studies of quantum thermodynamics [16–18].

Energy transfer in electron-phonon systems is the subject of intense and sustained research [19]. Time-resolved pump-probe spectroscopy is capable of tracking the non-equilibrium dynamics of electrons after excitation by a laser pulse. Predicting the subsequent phonon-induced electron relaxation is a challenge for existing theoretical approaches, and most work uses phenomenological models.

In this Letter, we derive Ehrenfest identities that can rigorously quantify the energy transfer between electrons and phonons. Our results, in fact, apply to any two-component system, though for concreteness we consider here a system of electrons and nuclei. Unlike conventional methods where quantum subsystems are described by a reduced density matrix [20,21] or nonequilibrium Green's function [22], the essence of our approach lies in the realization that a subsystem can be treated as a pure state whose dynamics are described by an effective Schrödinger equation.

Published by the American Physical Society under the terms of the [Creative Commons Attribution 4.0 International](https://creativecommons.org/licenses/by/4.0/) license. Further distribution of this work must maintain attribution to the author(s) and the published article's title, journal citation, and DOI. Open access publication funded by the Max Planck Society.

The exact factorization (EF) method [23–25] sets down the rigorous definition of a nuclear wave function that yields the exact nuclear probability density and current density [26]. We will show in this Letter that it also yields the exact nuclear angular momentum. The fact that the nuclear wave function obeys a TDSE in which all electronic effects have been condensed into scalar and vector potentials [24,25] is the key to point (ii) above, for it is precisely this structure that allows us to identify quantities with classical analogs in the subsystem Ehrenfest identities (SEIs) for the kinetic energy, momentum, and angular momentum.

Let us start with the full TDSE for electrons and nuclei,

$$i\partial_t\Psi(\underline{\mathbf{r}}, \underline{\mathbf{R}}, t) = \hat{H}\Psi(\underline{\mathbf{r}}, \underline{\mathbf{R}}, t), \quad (1)$$

where $\underline{\mathbf{r}} = (\mathbf{r}_1, \mathbf{r}_2, \dots, \mathbf{r}_{N_e})$ and $\underline{\mathbf{R}} = (\mathbf{R}_1, \mathbf{R}_2, \dots, \mathbf{R}_{N_n})$ denote the electronic and nuclear coordinates, respectively. \hat{H} is the full Hamiltonian which in the absence of external potentials comprises the nuclear kinetic energy \hat{T}_n , the electronic kinetic energy \hat{T}_e , electron-electron interaction \hat{V}_{ee} , electron-nucleus interaction \hat{V}_{en} , and nucleus-nucleus interaction \hat{V}_{nn} . The nuclear kinetic energy T_n , momentum \mathbf{P}_n , and angular momentum \mathbf{L}_n are defined as the expectation values of the corresponding operators,

$$T_n = \langle\Psi|\sum_{\mu=1}^{N_n} -\frac{1}{2M_\mu}\nabla_{\mathbf{R}_\mu}^2|\Psi\rangle_{\underline{\mathbf{r}}\underline{\mathbf{R}}}, \quad (2)$$

$$\mathbf{P}_n = \langle\Psi|\sum_{\mu=1}^{N_n} -i\nabla_{\mathbf{R}_\mu}|\Psi\rangle_{\underline{\mathbf{r}}\underline{\mathbf{R}}}, \quad (3)$$

$$\mathbf{L}_n = \langle\Psi|\sum_{\mu=1}^{N_n} \mathbf{R}_\mu \times (-i\nabla_{\mathbf{R}_\mu})|\Psi\rangle_{\underline{\mathbf{r}}\underline{\mathbf{R}}}. \quad (4)$$

Here, μ indexes the nuclei, M_μ are the nuclear masses, and the subscripts of the bra-kets indicate which variables are integrated over in the inner product. As a nonstationary Ψ evolves, these expectation values change in time due to the coupling to the electronic subsystem.

It has been shown that $\Psi(\underline{\mathbf{r}}, \underline{\mathbf{R}}, t)$ can be factorized into a marginal nuclear wave function $\chi(\underline{\mathbf{R}}, t)$ and a conditional electronic wave function $\Phi_{\underline{\mathbf{R}}}(\underline{\mathbf{r}}, t)$ [23–26]. Furthermore, $\Phi_{\underline{\mathbf{R}}}$ satisfies a complicated electronic equation while χ satisfies a simple nuclear TDSE [25,26], $i\partial_t\chi = \hat{H}_n\chi$, where $\hat{H}_n = \sum_{\mu=1}^{N_n} (1/2M_\mu)(-i\nabla_{\mathbf{R}_\mu} + \mathbf{A}_\mu)^2 + \epsilon$. Here, $\epsilon(\underline{\mathbf{R}}, t)$ is the scalar potential originating from the electronic equation, and $\mathbf{A}_\mu(\underline{\mathbf{R}}, t) = \langle\Phi_{\underline{\mathbf{R}}}| -i\nabla_{\mathbf{R}_\mu}|\Phi_{\underline{\mathbf{R}}}\rangle_{\underline{\mathbf{r}}}$ are nucleus-dependent vector potentials. By virtue of the fact that χ obeys a TDSE and can be viewed as the wave function of a

closed system acted on by ϵ and \mathbf{A}_μ , we can evaluate T_n , \mathbf{P}_n , and \mathbf{L}_n equally well as

$$T_n = \langle\chi|\sum_{\mu=1}^{N_n} \frac{1}{2M_\mu} (-i\nabla_{\mathbf{R}_\mu} + \mathbf{A}_\mu)^2|\chi\rangle_{\underline{\mathbf{R}}} + T_{n,\text{geo}}, \quad (5)$$

$$\mathbf{P}_n = \langle\chi|\sum_{\mu=1}^{N_n} (-i\nabla_{\mathbf{R}_\mu} + \mathbf{A}_\mu)|\chi\rangle_{\underline{\mathbf{R}}}, \quad (6)$$

$$\mathbf{L}_n = \langle\chi|\sum_{\mu=1}^{N_n} \mathbf{R}_\mu \times (-i\nabla_{\mathbf{R}_\mu} + \mathbf{A}_\mu)|\chi\rangle_{\underline{\mathbf{R}}}. \quad (7)$$

Here,

$$T_{n,\text{geo}} = \langle\chi|\sum_{\mu=1}^{N_n} \frac{1}{2M_\mu} (\langle\nabla_{\mathbf{R}_\mu} \Phi_{\underline{\mathbf{R}}}| \nabla_{\mathbf{R}_\mu} \Phi_{\underline{\mathbf{R}}}\rangle_{\underline{\mathbf{r}}} - A_\mu^2)|\chi\rangle_{\underline{\mathbf{R}}} \quad (8)$$

is an additional *geometric* term, which can be written as the tensor contraction of an inverse inertia tensor and a Riemannian metric measuring distance in the space of quantum states (see Ref. [27] and references therein.) Comparing Eqs. (5)–(7) with Eqs. (2)–(4), one can easily recognize their formal resemblance. The equivalence of Eq. (6) and Eq. (3) implies that the Ehrenfest equation for the momentum of the nuclei can be evaluated by considering either the full system or the nuclear subsystem alone, as shown in Ref. [28]. In replacing the full wave function Ψ by the marginal subsystem wave function χ and the corresponding integration domain, we obtain additional terms with vector potentials \mathbf{A}_μ arising in conjunction with the canonical momentum operators. A similar argument applies to the nuclear angular momentum. In contrast, Eq. (5) and Eq. (2) imply that the true nuclear kinetic energy T_n differs from the kinetic energy of the effective closed system described by the nuclear subsystem (marginal) TDSE, denoted as $T_{n,\text{marg}}$, by the quantity in Eq. (8) as shown in Ref. [29]. In the following, we derive the equations of motion for $T_{n,\text{marg}}$, \mathbf{P}_n , and \mathbf{L}_n , and will show that they all satisfy classical-like equations, governed by a unified force operator.

We start by applying the Heisenberg equation of motion for $T_{n,\text{marg}} = \langle\chi|\hat{T}_n|\chi\rangle$ with $\hat{T}_n = \sum_{\mu=1}^{N_n} (1/2M_\mu)(-i\nabla_{\mathbf{R}_\mu} + \mathbf{A}_\mu)^2$ to the nuclear TDSE, which leads to

$$\begin{aligned} \frac{dT_{n,\text{marg}}}{dt} &= i\langle\chi|[\hat{H}_n, \hat{T}_n]|\chi\rangle_{\underline{\mathbf{R}}} + \langle\chi|\frac{\partial\hat{T}_n}{\partial t}|\chi\rangle_{\underline{\mathbf{R}}} \\ &= \sum_{\mu=1}^{N_n} \frac{1}{M_\mu} \{ \langle\chi|(\partial_t \mathbf{A}_\mu - \nabla_{\mathbf{R}_\mu} \epsilon) \cdot (-i\nabla_{\mathbf{R}_\mu} + \mathbf{A}_\mu)|\chi\rangle_{\underline{\mathbf{R}}} \\ &\quad - i\frac{1}{2} \langle\chi|(\nabla_{\mathbf{R}_\mu} \cdot (\partial_t \mathbf{A}_\mu - \nabla_{\mathbf{R}_\mu} \epsilon))|\chi\rangle_{\underline{\mathbf{R}}} \}. \end{aligned} \quad (9)$$

Here, the left hand side of Eq. (9) is real. When we take the real part of Eq. (9), the left hand side stays the same while the second term in the braces of the right hand side vanishes since it is purely imaginary. Then, by introducing a velocity operator $\hat{\mathbf{v}}_\mu \equiv (1/M_\mu)(-i\nabla_{\mathbf{R}_\mu} + \mathbf{A}_\mu)$ for each nucleus and defining the effective electric field $\mathbf{E}_\mu = \partial_t \mathbf{A}_\mu - \nabla_{\mathbf{R}_\mu} \epsilon$, we condense Eq. (9) into the following compact form,

$$\frac{dT_{n,\text{marg}}}{dt} = \text{Re} \langle \chi | \sum_{\mu=1}^{N_n} \mathbf{E}_\mu \cdot \hat{\mathbf{v}}_\mu | \chi \rangle_{\underline{\mathbf{R}}}. \quad (10)$$

This equation is valid when there are no external forces driving the system. In the presence of external potentials acting on the electrons, those potentials will enter the electronic equation of motion leading to a modified electronic conditional wave function $\Phi_{\underline{\mathbf{R}}}(\underline{\mathbf{r}}, t)$ and hence to modified functions $A_\mu(\underline{\mathbf{R}}, t)$ and $\epsilon(\underline{\mathbf{R}}, t)$, but the form of Eq. (10) remains unchanged. On the other hand, external potentials acting on the nuclei will enter Eq. (10) directly through the replacements $A_\mu(\underline{\mathbf{R}}, t) \rightarrow A_\mu(\underline{\mathbf{R}}, t) + A_{\text{ext},\mu}(\underline{\mathbf{R}}, t)$ and $\epsilon(\underline{\mathbf{R}}, t) \rightarrow \epsilon(\underline{\mathbf{R}}, t) + v_{\text{ext}}(\underline{\mathbf{R}}, t)$.

Equation (10) casts the rate of change, $dT_{n,\text{marg}}/dt$, in the form of the classical work done per unit time by an electric field on a charged particle. We can obtain the rate of change of the full nuclear kinetic energy, dT_n/dt , by adding $dT_{n,\text{geo}}/dt$ to $dT_{n,\text{marg}}/dt$. A separate identity has been derived for $dT_{n,\text{geo}}/dt$ [30], but it cannot be expressed in a force-times-velocity form like Eq. (10).

In the absence of external forces, the total energy of the complete electron-nuclear system is conserved and can be written as the sum of three gauge-invariant terms: $E_{\text{tot}} = \langle \Psi(t) | \hat{H} | \Psi(t) \rangle_{\underline{\mathbf{R}}} = T_{n,\text{marg}}(t) + T_{n,\text{geo}}(t) + E_{\text{BO}}(t)$, where $E_{\text{BO}}(t) = \langle \Psi(t) | \hat{T}_e + \hat{V}_{ee} + \hat{V}_{en} + \hat{V}_{nn} | \Psi(t) \rangle_{\underline{\mathbf{R}}}$ is the Born-Oppenheimer (BO) energy contribution. As we will demonstrate in the later sections of this Letter, nonadiabatic dynamical processes can be efficiently analyzed in terms of the energy transfer between these three gauge-invariant quantities (even when external forces are present). It will turn out that $T_{n,\text{geo}}$ is sizable, when a nonadiabatic population transfer between BO surfaces occurs. On the other hand, in the extreme adiabatic limit, when the factorization of the total wave function reduces to $\Psi(\underline{\mathbf{r}}, \underline{\mathbf{R}}, t) = \chi(\underline{\mathbf{R}}, t) \Phi_{\text{BO}}(\underline{\mathbf{r}} | \underline{\mathbf{R}})$, i.e., to a vibrational wave packet $\chi(\underline{\mathbf{R}}, t)$ oscillating in a single BO surface, then $T_{n,\text{geo}}$ tends to be small, and one mainly observes the periodic energy transfer between $T_{n,\text{marg}}(t)$ and $E_{\text{BO}}(t)$, i.e., the transfer between kinetic and potential energy of the oscillating wave packet. The expectation value $\langle \chi(t) | \hat{H}_n | \chi(t) \rangle_{\underline{\mathbf{R}}}$ of the nuclear subsystem Hamiltonian is not gauge invariant. However, interestingly, in the particular gauge defined by $\langle \Phi_{\underline{\mathbf{R}}}(\underline{\mathbf{r}}, t) | i\partial_t | \Phi_{\underline{\mathbf{R}}}(\underline{\mathbf{r}}, t) \rangle_{\underline{\mathbf{r}}} = 0$ (which is the natural gauge

when the electronic factor is identical with a static BO state), $\langle \chi(t) | \hat{H}_n | \chi(t) \rangle_{\underline{\mathbf{R}}}$ becomes identical with E_{tot} , suggesting that the periodic exchange between kinetic and potential energy of the marginal subsystem can be interpreted as periodic energy transfer between electrons and nuclei.

Next, we derive the SEI for the nuclear momentum. Here, instead of summing up the momenta of all nuclei, let us consider each individual $\mathbf{P}_\mu = \langle \chi | \hat{\mathbf{p}}_\mu | \chi \rangle_{\underline{\mathbf{R}}}$, where $\hat{\mathbf{p}}_\mu = -i\nabla_{\mathbf{R}_\mu} + \mathbf{A}_\mu$. Once again, we use the Heisenberg equation of motion to arrive at

$$\begin{aligned} \frac{d\mathbf{P}_\mu}{dt} &= i \langle \chi | [\hat{H}_n, \hat{\mathbf{p}}_\mu] | \chi \rangle_{\underline{\mathbf{R}}} + \langle \chi | \partial_t \hat{\mathbf{p}}_\mu | \chi \rangle_{\underline{\mathbf{R}}} \\ &= \langle \chi | \mathbf{E}_\mu | \chi \rangle_{\underline{\mathbf{R}}} + i \langle \chi | [\hat{t}_n, \hat{\mathbf{p}}_\mu] | \chi \rangle_{\underline{\mathbf{R}}}. \end{aligned} \quad (11)$$

Let us denote $\mathbf{Q}_\mu = i \langle \chi | [\hat{t}_n, \hat{\mathbf{p}}_\mu] | \chi \rangle_{\underline{\mathbf{R}}}$. The fact that $d\mathbf{P}_\mu/dt$ and $\langle \chi | \mathbf{E}_\mu | \chi \rangle_{\underline{\mathbf{R}}}$ are both real implies \mathbf{Q}_μ is real. By some algebra, we derive the G ($G = X, Y, Z$) component of \mathbf{Q}_μ as given by

$$\begin{aligned} Q_\mu^G &= \text{Re} \langle \chi | \sum_{\nu G'} (\partial_{G'_\nu} A_{G_\mu} - \partial_{G_\mu} A_{G'_\nu}) \hat{v}_{G'_\nu} | \chi \rangle_{\underline{\mathbf{R}}} \\ &= \text{Re} \langle \chi | \sum_{\nu G'} C_{\nu\mu}^{G'G} \hat{v}_{G'_\nu} | \chi \rangle_{\underline{\mathbf{R}}}. \end{aligned} \quad (12)$$

Here, $C_{\nu\mu}^{G'G} \equiv \partial_{G'_\nu} A_{G_\mu} - \partial_{G_\mu} A_{G'_\nu}$ is the Berry curvature. By grouping Q_μ^G into intranuclear and internuclear contributions,

$$Q_\mu^G = \text{Re} \langle \chi | \sum_{G'} \left(C_{\mu\mu}^{G'G} \hat{v}_{G'_\mu} + \sum_{\nu \neq \mu} C_{\nu\mu}^{G'G} \hat{v}_{G'_\nu} \right) | \chi \rangle_{\underline{\mathbf{R}}}, \quad (13)$$

we can identify some classical analogs. In particular, the intranuclear curvature $C_{\mu\mu}^{G'G}$ behaves like a classical magnetic field \mathbf{B}_μ , where $C_{\mu\mu}^{XY} = B_\mu^Z$, $C_{\mu\mu}^{YZ} = B_\mu^X$, and $C_{\mu\mu}^{ZX} = B_\mu^Y$. Upon summing over G' , these intranuclear terms lead to the following simple expression:

$$\sum_{G'} C_{\mu\mu}^{G'G} \hat{v}_{G'_\mu} = (\mathbf{B}_\mu \times \hat{\mathbf{v}}_\mu)_G. \quad (14)$$

The classical counterpart of Eq. (14) is the magnetic force acting on nucleus μ , which combined with \mathbf{E}_μ in Eq. (11) leads to the generalized Lorentz force operator

$$\hat{\mathbf{F}}_\mu = \mathbf{E}_\mu + \mathbf{B}_\mu \times \hat{\mathbf{v}}_\mu. \quad (15)$$

In contrast to the classical picture, here this force is an operator and the electromagnetic field is nucleus specific. Moreover, the appearance of the magnetic force as $\mathbf{B}_\mu \times \hat{\mathbf{v}}_\mu$ rather than $-\mathbf{B}_\mu \times \hat{\mathbf{v}}_\mu$ occurs because the sign in our definition of \mathbf{A}_μ is the opposite of that in the conventional

definition [31], which flips the sign of A_μ in the definition of $\hat{\mathbf{p}}_\mu$.

On the other hand, the summation over the internuclear curvature terms has no classical analog and does not readily simplify. Instead, we introduce an internuclear magnetic force operator

$$\hat{D}_\mu^G = \sum_{\nu \neq \mu, G'} C_{\nu\mu}^{G'G} \hat{v}_{G'} = \sum_{\nu \neq \mu} (\nabla_{\mathbf{R}_\nu} A_{G_\mu} - \partial_{G_\mu} A_\nu) \cdot \hat{v}_\nu. \quad (16)$$

The internuclear Berry curvature $C_{\nu\mu}^{G'G}$ has been studied previously in the BO approximation [32,33]. Eq. (11) simplifies to the following SEI:

$$\frac{d\mathbf{P}_\mu}{dt} = \text{Re}\langle \chi | \hat{\mathbf{F}}_\mu + \hat{D}_\mu | \chi \rangle_{\underline{\mathbf{R}}} \equiv \text{Re}\langle \chi | \hat{\mathcal{F}}_\mu | \chi \rangle_{\underline{\mathbf{R}}}. \quad (17)$$

Here, $\hat{\mathcal{F}}_\mu \equiv \hat{\mathbf{F}}_\mu + \hat{D}_\mu$ denotes the electromagneticlike *force operator* whose expectation value gives the mean force on nucleus μ . Our $\hat{\mathcal{F}}_\mu$ has a formal resemblance to the classical force function F_μ^I that was introduced in previous works for calculating the time evolution of the nuclear momentum \mathbf{P}_μ^I of a particular trajectory $\underline{\mathbf{R}}^I(t)$ in a trajectory-based representation of the nuclear Schrödinger equation [34–39]. In fact, one can show that $\mathbf{P}_\mu^I \equiv \mathbf{P}_\mu(\underline{\mathbf{R}}^I(t), t) = \text{Re}(\hat{\mathbf{p}}_\mu \chi / \chi)|_{\underline{\mathbf{R}}=\underline{\mathbf{R}}^I(t)}$ and $F_\mu^I \equiv F_\mu(\underline{\mathbf{R}}^I(t), t) = \text{Re}(\hat{\mathcal{F}}_\mu \chi / \chi)|_{\underline{\mathbf{R}}=\underline{\mathbf{R}}^I(t)}$. Although \mathbf{P}_μ^I and F_μ^I are auxiliary quantities tied to the trajectory based methods, where $\underline{\mathbf{R}}$ and t are no longer independent variables, one expects to recover $d\mathbf{P}_\mu/dt$ upon taking the ensemble average. In this Letter, we have derived a representation independent identity for the rate of change of the observable $\langle \chi | \hat{\mathbf{p}}_\mu | \chi \rangle$, showing that it is governed by the novel force operator on the right hand side of Eq. (17). Interestingly, the right hand side can be evaluated in the position representation by replacing $\hat{\mathcal{F}}_\mu$ by $F_\mu(\underline{\mathbf{R}}, t)$ due to the formal resemblance of these forces, see [40] and example below.

Next, we show that the same force operator appears in the equations of motion for \mathbf{L}_μ and $T_{n,\text{marg}}$. By following a similar derivation, we can connect the rate of change of angular momentum with an effective torque [40],

$$\frac{d\mathbf{L}_\mu}{dt} = \text{Re}\langle \chi | \mathbf{R}_\mu \times \hat{\mathcal{F}}_\mu | \chi \rangle_{\underline{\mathbf{R}}}. \quad (18)$$

On the contrary, such a simple relation does not hold for kinetic energy of an individual nucleus, i.e., $dT_{\mu,\text{marg}}/dt \neq \text{Re}\langle \chi | \hat{\mathcal{F}}_\mu \cdot \hat{v}_\mu | \chi \rangle_{\underline{\mathbf{R}}}$. Replacing $\hat{\mathcal{F}}_\mu$ by $\hat{\mathbf{F}}_\mu$ or \mathbf{E}_μ does not lead to the right formula either. Only by summing over all nuclei can we achieve an equality involving $\hat{\mathcal{F}}_\mu$ [40],

$$\frac{dT_{n,\text{marg}}}{dt} = \text{Re}\langle \chi | \sum_{\mu=1}^{N_n} \hat{\mathcal{F}}_\mu \cdot \hat{v}_\mu | \chi \rangle_{\underline{\mathbf{R}}}. \quad (19)$$

Equations (10) and (19) imply that the magneticlike forces do no work. One can immediately see this for the intranuclear magnetic force because $(\mathbf{B}_\mu \times \hat{v}_\mu) \cdot \hat{v}_\mu = 0$. On the other hand, although each $\text{Re}\langle \chi | \hat{D}_\mu \cdot \hat{v}_\mu | \chi \rangle$ is non-zero, they compensate one another upon summation due to the internal nature of the force \hat{D}_μ .

To visualize the SEIs, we design an exactly solvable model of two nuclei moving in one dimension. Let us assume that the information of the electron-nuclear wave function Ψ has been condensed into a nuclear wave function χ that satisfies the following TDSE:

$$i\partial_t \chi = \frac{1}{2M} \sum_{\mu=1}^2 (-i\partial_{X_\mu} + A_\mu)^2 \chi + \epsilon \chi. \quad (20)$$

Although Ψ is a complex function, we can always choose a gauge such that χ is real. Here, instead of following the conventional way of solving for χ with given time dependent scalar and vector potentials and initial condition, we go the other way around. By choosing a particular form of time-evolving wave function $\chi(X_1, X_2, t)$, we aim to find analytical forms of the corresponding A_1 , A_2 , and ϵ as functions of X_1 , X_2 , and t that yield such a χ . In this work, we choose χ to be a normalized Gaussian function of a fixed width σ ,

$$\chi(X_1, X_2, t) = \frac{1}{\sigma\sqrt{\pi}} \exp\left\{-\frac{1}{2\sigma^2} \sum_{\mu=1}^2 [X_\mu - g_\mu(t)]^2\right\}, \quad (21)$$

whose center moves along a trajectory $[g_1(t), g_2(t)]$. Taking the real part of Eq. (20), and using the fact that χ is chosen to be real, we can deduce the form of ϵ in terms of χ and A_μ . Here, we choose the following vector potentials yielding χ :

$$A_1(X_1, X_2, t) = f(t)[-X_2 + g_2(t)] + Mg_1'(t), \quad (22)$$

$$A_2(X_1, X_2, t) = f(t)[X_1 - g_1(t)] + Mg_2'(t), \quad (23)$$

where $f(t)$ and g_μ are periodic functions in time, yielding a spiral nuclear center trajectory (see [40] for details).

Because the nuclei move in one dimension, the intranuclear magnetic field B is absent so that the generalized Lorentz force reduces to the electromotive force $F_\mu = E_\mu$. However, propagating the Newton's equation with only this force $\bar{F}_\mu = \langle \chi | F_\mu | \chi \rangle$ will lead to an incorrect trajectory for the center of the nuclear wave packet. Because of the presence of a nonzero internuclear Berry curvature $C_{12} = \partial_{X_1} A_2 - \partial_{X_2} A_1 = 2f(t)$, the internuclear magnetic force operators $\hat{D}_1 = -C_{12}\hat{v}_2$ and $\hat{D}_2 = C_{12}\hat{v}_1$ contribute to

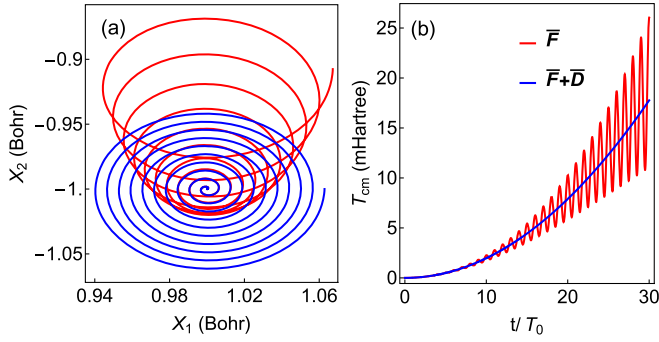


FIG. 1. (a) Trajectory of the center of the nuclear wave packet shown as a 2D plot. The initial position is at $(1, -1)$. With the incomplete force \bar{F} , the nuclear center deviates from the correct spiral trajectory after a few cycles. (b) Center of mass kinetic energy T_{cm} as a function of t calculated with \bar{F} and $\bar{F} + \bar{D}$. Here, $T_0 = 6.8$ fs is the time period.

the correct force $\bar{F}_\mu + \bar{D}_\mu = \text{Re}\langle\chi|F_\mu + \hat{D}_\mu|\chi\rangle$ acting on the nuclear wave packet.

This is illustrated in Fig. 1(a), where we compare trajectories generated by the exact and incomplete mean force. As can be seen, the exact force drives the nuclear center to swirl around its initial position, while the incomplete force produces a spurious acceleration of the second nucleus in the X direction. Although the missing \hat{D}_μ contributions are small relative to \hat{F}_μ (see [40]), its cumulative effect in time can be sizable. After ten cycles, this leads to a net displacement of X_2 of about 0.1 Bohr. In molecular dynamics, the size of \hat{D}_μ and its relative importance are unknown and deserve further study.

Next, let us consider the kinetic energy change during this swirling process. By direct computation, the kinetic energy increase over the initial time is

$$T_{n,\text{marg}}(t) - T_{n,\text{marg}}(0) = \frac{1}{2M} \sigma^2 f^2(t) + \frac{1}{2} M \bar{v}^2. \quad (24)$$

Here, the first term on the right hand side of Eq. (24) is purely a quantum effect. If we assume that the nuclear wave packet is narrow and $f(t)$ is small, this term is only of secondary importance. By contrast, the dominant term is the second one, where $\bar{v} = [g'_1(t), g'_2(t)]$ is the velocity of the nuclear center of mass and $\frac{1}{2} M \bar{v}^2 \equiv T_{\text{cm}}$ is the classical nuclear kinetic energy. In Fig. 1(b), we compare T_{cm} using the trajectories generated by the exact and incomplete forces. As shown, the incomplete force yields T_{cm} with artificial oscillations around the exact curve.

Our model has great similarity with the current-driven atomic water wheel model studied in [8], if we interpret X_1 and X_2 as two Cartesian coordinates of the same nucleus. We emphasize that $\bar{F} + \bar{D}$ is the key quantity that determines the stability and working efficiency of the water wheel, see [40] for further discussions.

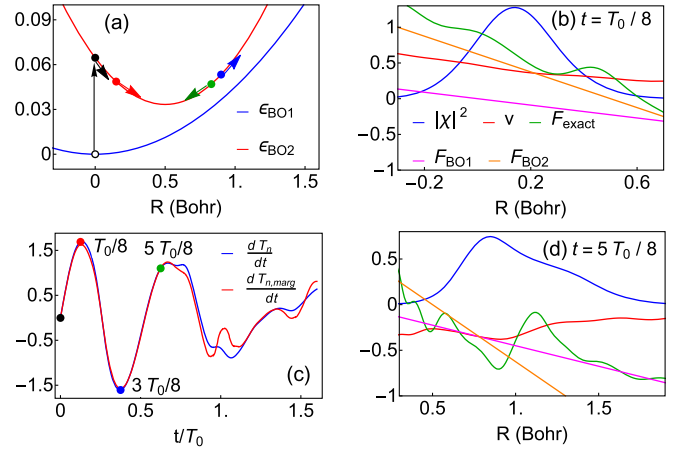


FIG. 2. (a) BO surfaces (in Hartree) with illustrative dots and arrows indicating the nuclear vibration after a vertical excitation. (b) $|\chi|^2$, $v = \text{Re}(\hat{v}\chi/\chi)$, and the exact force function in atomic units evaluated at $t = T_0/8$, where $T_0 = 13.6$ fs. Forces from the static BO surfaces are also shown as reference curves. To put all these curves in one figure, $|\chi|^2$ has been scaled by a factor of $\frac{1}{2}$, v by a factor of 100 and all the forces by a factor of 5. (c) Rate of change of T_n and $T_{n,\text{marg}}$ as functions of time in unit of 10^{-2} Hartree/fs. Chosen instants of time are marked by colored dots corresponding to the ones in (a). (d) same as in (b) except evaluated at $t = 5T_0/8$.

In Fig. 2, we also simulate the energy transfer between electrons and nuclei after a vertical excitation to an excited electronic state in a two-level model diatomic molecule (details can be found in Supplemental Material [40]). This is related to the early stage of a bond-breaking process [41], particularly the reaction pathways of small molecules [42], or the redistribution of energy of DNA and RNA [2,3]. Here, we idealize the two BO surfaces as harmonic potentials with an avoided crossing in the region $R = 0.5-1$ Bohr. As illustrated in Fig. 2(a), after vertical excitation from the equilibrium position of the lower surface, the nuclear wave packet χ starts propagating on the upper one. If we neglect the coupling of the two surfaces, χ undergoes perfect harmonic oscillations around $R = 0.5$ Bohr with a time period $T_0 = 13.6$ fs. However, because of the coupling of the surfaces, the nuclear wave packet splits into two branches as it goes through the avoided crossing. One branch stays on the upper surface while the other transfers to the lower one accompanied by energy transfer from electrons to the nuclear kinetic energy. This process also breaks the time periodicity because the split wave packets feel the gradients (forces) of two different BO potentials. This is also reflected in Fig. 2(c), where the rate of change of $T_{n,\text{marg}}$ and T_n as functions of t deviate from periodic behavior when $t > T_0/2$. Here, we focus on two points, $t = T_0/8$ and $t = 5T_0/8$, roughly corresponding to the first two maxima. As shown, there is a significant decrease in $dT_{n,\text{marg}}/dt$ from $t = T_0/8$ to $t = 5T_0/8$. To understand this change, we use our identity (19) and rewrite it as

$$\frac{dT_{n,\text{marg}}}{dt} = \int |\chi(R, t)|^2 F(R, t) v(R, t) dR, \quad (25)$$

where we introduce a velocity function $v(R, t) = \text{Re}(\hat{v}\chi/\chi)$. In Figs. 2(b) and 2(d) we compare $|\chi|^2$, F , and v at the chosen times. As shown, in (d) $|\chi|^2$ is broadened; and in the region where $|\chi|^2$ is large, the exact F and v become smaller in absolute value although they change sign as a result of the reversal of the moving direction. All of these changes contribute to the drop of $dT_{n,\text{marg}}/dt$ at $t = 5T_0/8$.

As a side remark, the relative importance of $dT_{n,\text{geo}}/dt$ can be deduced from Fig. 2(c). It is unimportant for $t < (5T_0/8)$ but starts to build up when χ repeatedly traverses the nonadiabatic region. The example shown here corresponds to an intermediate nonadiabatic coupling regime. In the adiabatic regime, the effect of $T_{n,\text{geo}}$ becomes much smaller. Discussions on this along with the electronic energy and population transfer in adiabatic regimes are presented in Supplemental Material [40].

To better understand the exact force function, we compare it with the forces calculated from the BO surfaces, which are straight lines in Figs. 2(b) and 2(d). As shown in (b), the exact force has similar slope with $F_{\text{BO}2}$, although amplified by quantum corrections. In (d), however, it follows the slope of $F_{\text{BO}1}$ for $R < 1$ Bohr while turning to follow $F_{\text{BO}2}$ for $R > 1$ Bohr, suggesting a split of the nuclear wave packet at $R = 1$ Bohr, as also indicated by the emerging shoulder in $|\chi|^2$. Our observation of the piecewise behavior in the exact force in case of wave packet splitting is also in line with the literature [29].

To summarize, in this Letter we have used the nuclear TDSE of the exact factorization method to establish subsystem Ehrenfest identities for the three main canonical variables in classical and quantum mechanics. We have shown that the same effective electromagnetic force operator $\hat{\mathcal{F}}_\mu$ appears in all three identities. The magnetic component of the corresponding electromagnetic field comes from two sources: (a) the more familiar intranuclear Berry curvature associated with different Cartesian coordinates of the same nucleus [31]; (b) the internuclear Berry curvature calculated with arbitrary Cartesian coordinates of two different nuclei. (a) has the classical interpretation of an effective magnetic field acting on a given nucleus, while (b) has no classical analog. In practical calculations, one can take advantage of the recently developed exact factorization-based density functional theory [43–46] to evaluate these forces as functionals of the conditional electronic density and nuclear probability density. One can also apply the approximate Born-Oppenheimer factorization to derive the same SEIs for approximate forces. By condensing the enormous amount of information in the electron-nuclear wave function into comprehensible quantities such as force and velocity, we will gain more insight into dynamical processes on the atomic scale.

We thank Ali Abedi and Federica Agostini for helpful discussions. This project has received funding from the European Research Council (ERC) under the European Unions Horizon 2020 research and innovation programme (Grant Agreement No. ERC-2017-AdG-788890). E. K. U. Gross acknowledges support as Mercator Fellow within SFB 1242 at the University Duisburg-Essen.

*chenlichem@pku.edu.cn

- [1] P. Ehrenfest, *Z. Phys.* **45**, 455 (1927).
- [2] J.-M. L. Pecourt, J. Peon, and B. Kohler, *J. Am. Chem. Soc.* **123**, 10370 (2001).
- [3] J. Peon and A. H. Zewail, *Chem. Phys. Lett.* **348**, 255 (2001).
- [4] R. J. Maurer, M. Askerka, V. S. Batista, and J. C. Tully, *Phys. Rev. B* **94**, 115432 (2016).
- [5] M. Hopjan, G. Stefanucci, E. Perfetto, and C. Verdozzi, *Phys. Rev. B* **98**, 041405 (2018).
- [6] C. Martinazzo and I. Burghardt, arXiv:2108.02622v2.
- [7] M. Di Ventra, S. Pantelides, and N. Lang, *Phys. Rev. Lett.* **88**, 046801 (2002).
- [8] D. Dundas, E. J. McEniry, and T. N. Todorov, *Nat. Nanotechnol.* **4**, 99 (2009).
- [9] T. N. Todorov, D. Dundas, J.-T. Lü, M. Brandbyge, and P. Hedegård, *Euro. J. Phys.* **35**, 065004 (2014).
- [10] A. P. Horsfield, D. Bowler, A. Fisher, T. N. Todorov, and M. Montgomery, *J. Phys. Condens. Matter* **16**, 3609 (2004).
- [11] A. P. Horsfield, D. Bowler, H. Ness, C. Sánchez, T. N. Todorov, and A. Fisher, *Rep. Prog. Phys.* **69**, 1195 (2006).
- [12] F. Jülicher, A. Ajdari, and J. Prost, *Rev. Mod. Phys.* **69**, 1269 (1997).
- [13] E. R. Kay, D. A. Leigh, and F. Zerbetto, *Angew. Chem.* **46**, 72 (2007).
- [14] J. Chen, F. K.-C. Leung, M. C. Stuart, T. Kajitani, T. Fukushima, E. van der Giessen, and B. L. Feringa, *Nat. Chem.* **10**, 132 (2018).
- [15] K. H. Kim and H. Qian, *Phys. Rev. E* **75**, 022102 (2007).
- [16] R. Alicki, *J. Phys. A* **12**, L103 (1979).
- [17] R. Kosloff, *J. Chem. Phys.* **80**, 1625 (1984).
- [18] R. Kosloff, *Entropy* **15**, 2100 (2013).
- [19] P. Maldonado, T. Chase, A. H. Reid, X. Shen, R. K. Li, K. Carva, T. Payer, M. Horn von Hoegen, K. Sokolowski-Tinten, X. J. Wang, P. M. Oppeneer, and H. A. Dürr, *Phys. Rev. B* **101**, 100302 (2020).
- [20] S. Nakajima, *Prog. Theor. Phys.* **20**, 948 (1958).
- [21] R. Zwanzig, *J. Chem. Phys.* **33**, 1338 (1960).
- [22] L. P. Kadanoff and G. Baym, *Quantum Statistical Mechanics* (Benjamin, New York, 1962).
- [23] G. Hunter, *Int. J. Quantum Chem.* **9**, 237 (1975).
- [24] N. I. Gidopoulos and E. K. U. Gross, *Phil. Trans. R. Soc. A* **372**, 20130059 (2014).
- [25] A. Abedi, N. T. Maitra, and E. K. U. Gross, *Phys. Rev. Lett.* **105**, 123002 (2010).
- [26] A. Abedi, N. T. Maitra, and E. K. U. Gross, *J. Chem. Phys.* **137**, 22A530 (2012).
- [27] R. Requist, F. Tandetzky, and E. K. U. Gross, *Phys. Rev. A* **93**, 042108 (2016).

- [28] F. Agostini, A. Abedi, Y. Suzuki, and E. K. U. Gross, *Mol. Phys.* **111**, 3625 (2013).
- [29] F. Agostini, A. Abedi, Y. Suzuki, S. K. Min, N. T. Maitra, and E. K. U. Gross, *J. Chem. Phys.* **142**, 084303 (2015).
- [30] R. Requist, C. Li, and E. K. U. Gross, [arXiv:2112.08694v1](https://arxiv.org/abs/2112.08694v1) [Phil. Trans. R. Soc. A].
- [31] M. V. Berry, in *Geometric Phases in Physics* (World Scientific, Singapore, 1989), pp. 7–28.
- [32] D. Ceresoli, R. Marchetti, and E. Tosatti, *Phys. Rev. B* **75**, 161101(R) (2007).
- [33] J.-T. Lü, M. Brandbyge, and P. Hedegård, *Nano Lett.* **10**, 1657 (2010).
- [34] A. Abedi, F. Agostini, and E. K. U. Gross, *Europhys. Lett.* **106**, 33001 (2014).
- [35] F. Agostini, A. Abedi, and E. K. U. Gross, *J. Chem. Phys.* **141**, 214101 (2014).
- [36] S. K. Min, F. Agostini, and E. K. U. Gross, *Phys. Rev. Lett.* **115**, 073001 (2015).
- [37] F. Agostini, S. K. Min, A. Abedi, and E. K. U. Gross, *J. Chem. Theory Comput.* **12**, 2127 (2016).
- [38] B. F. E. Curchod, F. Agostini, and I. Tavernelli, *Euro. Phys. J. B* **91**, 168 (2018).
- [39] F. Agostini, I. Tavernelli, and G. Ciccotti, *Euro. Phys. J. B* **91**, 139 (2018).
- [40] See Supplemental Material at <http://link.aps.org/supplemental/10.1103/PhysRevLett.128.113001> for our derivations and model problems.
- [41] K. Cao, S. T. Skowron, J. Biskupek, C. T. Stoppiello, C. Leist, E. Besley, A. N. Khlobystov, and U. Kaiser, *Sci. Adv.* **6**, eaay5849 (2020).
- [42] Y. Xie, H. Zhao, Y. Wang, Y. Huang, T. Wang, X. Xu, C. Xiao, Z. Sun, D. H. Zhang, and X. Yang, *Science* **368**, 767 (2020).
- [43] C. Li, R. Requist, and E. K. U. Gross (to be published).
- [44] R. Requist, C. R. Proetto, and E. K. U. Gross, *Phys. Rev. B* **99**, 165136 (2019).
- [45] C. Li, R. Requist, and E. K. U. Gross, *J. Chem. Phys.* **148**, 084110 (2018).
- [46] R. Requist and E. K. U. Gross, *Phys. Rev. Lett.* **117**, 193001 (2016).